Single Feed Dual-Polarization Dual-Band Transmitarray for Satellite Applications

S. Zainud-Deen, S. Gaber,H. Malhat, and K. Awadalla

Department of Electronics and Electrical Communications Engineering,
Faculty of Electronic Engineering, Menoufiya University, Egypt
anssaber@yahoo.com, er_honida1@yahoo.com

***Abstract*—**In this paper, two transmitarrays are designed, analyzed, and simulated for satellite applications. The first transmitarray is designed for dual linear polarization at a center frequency of 12 GHz. The second transmitarray is designed for two frequency bands: 17.15 GHz to 17.9 GHz for vertical polarization and 11.5 GHz to 12.4 GHz for horizontal polarization. The dual polarization is obtained by an independent adjustment of the dimensions of two orthogonal slots in the transmitarray unit cell. The design is carried out independently for each polarization. The transmitarray unit cell uses two dielectric substrate layers arranged to be one on each side of a conducting plane. On each substrate, one face has metallization containing the patches, and the other face has metallization containing the ground plane. The two patches are coupled by two cross slots of lengths L_V and L_H in the ground plane and each patch is loaded with two cross slots of lengths $L_V/2$ and $L_H/2$. The unit cell achieves 360^o of phase agility with less than 3.8 dB of variation in the transmission magnitude in the tuning range. The transmitarray consisted of 17×17 elements with the unit cell size were set at 13 mm. A circular feed horn is located on the central normal to the transmitarray and the configuration looks like a lens antenna. Two separate feeding pins are used to excite the horn antenna for horizontal and vertical polarizations. The results are worked out using two basically different numerical techniques, the finite element method, FEM, and the finite integration technique, FIT. Good agreement was obtained.

***Index Terms* —** DRA, dual-band, Polarization, and Transmitarray.

I. INTRODUCTION

Transmitarray antenna is a good candidate for high-gain and broadband performance. It also has the privileges of light-weight, simple to fabricate, and inexpensive to manufacture [1]. As a high gain antenna, it is suitable for applications, such as radar, satellite communications, and remote sensing. The transmitarray performance is related to lens techniques. Its size and weight are advantages relative to shaped dielectric lenses. Furthermore, its feed can be placed directly in front of the aperture without causing blockage losses or affecting the radiation patterns that are inherent in a reflectarray configuration [1]. The objective of the transmitarray unit cell is to add a phase shift to the waves passing it, such that the phase shift should become adjustable in the range of 0 to 360^o. The main drawback of the transmitarray is its limited bandwidth, which is mainly due to the limited bandwidth of the element itself [2]. A number of different transmitarray configurations have been reported in the literature. These configurations can be classified according to the techniques that were used to adjust the phase of the incoming wave. Transmitarrays were designed using stub-loaded microstrip patches [3], and others using elements connected through multiple layers by a delay line [4]. A broadband four-layer transmitarray using double square printed ring elements is illustrated in [1].

A design of multilayer dielectric resonator transmitarray for near-field and far-field fixed RFID reader application at 5.8 GHz is presented in [5]. A three-layer printed reflectarray for dual polarization with different coverage in each polarization for space applications has been designed and tested in [6]. Also, a new application

Submitted On: October 15, 2012
Accepted On: January 26, 2014

of aperture coupled dielectric resonator as a cell element in design of a dual linear polarized reflectarray at X-band is investigated in [7]. A dual linear polarized printed reflectarray using slot loaded patch elements is investigated in [8]. The goal of this paper is to design a dual-polarization dual-band transmitarray. Two transmitarrays are simulated. The first transmitarray is designed for dual polarization at 12 GHz. The second transmitarray is designed for two frequency bands: 17.15 GHz to 17.9 GHz for vertical polarization and 11.5 GHz to 12.4 GHz for the horizontal polarization. The results are developed using finite element method [9] and compared with that determined using the basically different finite integration technique [10].In this work a single feed horn is used for horizontal and vertical polarization at different frequency bands instead of dual feeds used in [7, 8]. The two orthogonal linear polarizations can be controlled independently by using two orthogonal slots in the cell element. The slot lengths are used to control the transmission phase. For dual band operation, each of the orthogonal slots is designed to resonant at one of the two considered frequency bands.

II. THE CELL ELEMENT

The cell element in a transmitarray is the crucial part, which determines most of the parameters of the array. The cell is that, which controls the bandwidth, the polarization, and the transmission coefficient of the array. The cell should provide the amplitude and phase shift needed at each location in the array to produce the specific radiation in the specific direction. To reach full flexibility in getting the radiation in any specific direction, the cell element should be able to add any needed phase shift in the range from 0° to 360°. The unit cell is designed for having transmission phase variation from 0° to 360° with corresponding transmission magnitude variation from 0 to nearly -3 dB. The unit cell design process is go for this goal.

A thin dielectric slab will produce a constant phase shift of the order of several degrees (around 2 or 3 degrees). A slotted ground plane between two dielectric slabs will produce a phase shift ranging from 0° to about 175° depending upon the length of the slot as given in Fig. 1. To increase the phase shift of the transmitted wave a conducting square patch is added on one side face of the slab and centered with the ground slot. This actually made things worse and reduced the phase shift by about 20°. Then adding a slot on the patch parallel to the ground slot and centered with it but of half its length has improved the phase shift by adding 100° to that of the ground slot to reach about 280° maximum as shown in Fig. 2. This structure can be represented as two sections of waveguides connected in tandem to produce a delay of 280° for a travelling wave. To achieve the 360° needed, a third section of a waveguide is added in tandem. This is done by adding a similar slotted patch on the opposite face of the composite dielectric to end up with the cell element shown in Fig. 3. This completes the cell structure with three slotted elements on top of each other (in tandem) and in a symmetrical way on the same axis to add the phase shift of each section to end up with the needed 360° as shown in Fig. 3. Thus, by changing the length of the slots, the needed phase shift at each location in the array is obtained. The length of the ground slot is changed but with keeping the length of the slots on the patches to be half the accompanying ground slot length. The total response of the complete cell becomes similar to critical coupling in inductive coupled tuned circuits.

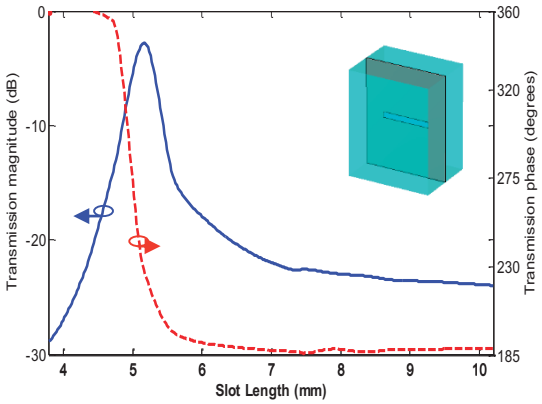

Fig. 1. A slotted ground plane sandwiched between two dielectric slabs.

To get the cell responding in a similar way to two orthogonal linearly polarized waves, identical slots orthogonal to the first ones is added on both patches on the two outer faces as well as on the ground plane to end up with the cell structure shown in Fig. 4. As expected, due to the

orthogonality of the slots, there is no mutual effect has been noticed between the orthogonal groups of slots sharing the same cell.

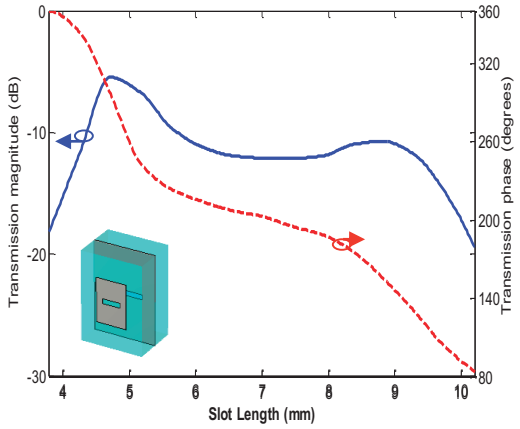

Fig. 2. The transmission coefficient after adding the slotted patch.

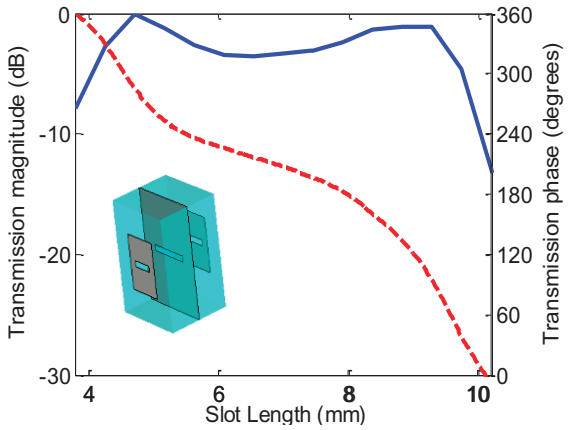

Fig. 3. The complete cell structure for one polarization.

III. STRUCTURE, SIMULATION, AND NUMERICAL RESULTS

A. Case A: Dual-polarization transmitarray at 12 GHz

Figure 4 depicts the layer distribution and materials employed in the transmitarray unit cell. It consists of two patches on either side of a ground plane, coupled by two cross slots of lengths L_V and L_H in the ground plane. Each patch is loaded with two cross slots of lengths $L_V/2$ and $L_H/2$. The slot widths were set at $W_v=W_H$ =0.7 mm. The transmitarray unit cell uses two substrate layers with $\varepsilon_r = 4$(Eccostock HIK500F). The unit cell size (L) was set at 13 mm. The cell dimensions are summarized in Table I. these dimensions are optimized to give transmission phase of 360° at the center frequency with maximum transmission magnitude.

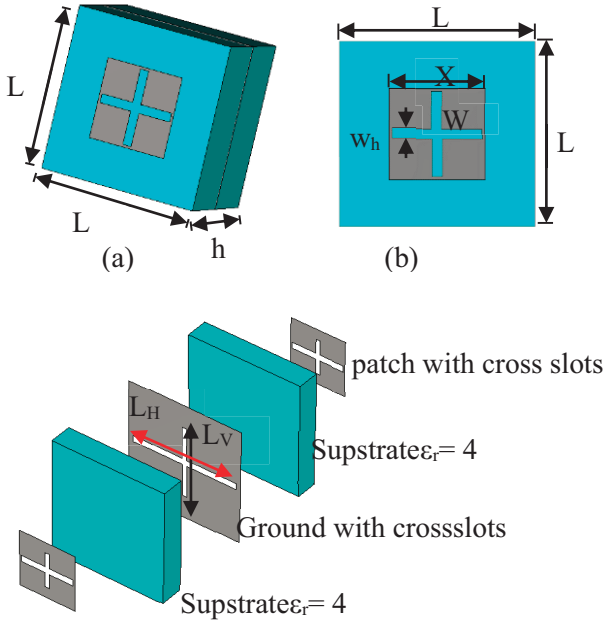

Fig. 4. Reconfigurable transmitarray element structure.

Table I: The unit cell dimensions

L	X	h	Slot width $W_v = W_H$
13 mm	6 mm	2.5 mm	0.7 mm

The transmission magnitude and phase are determined using the finite element method based simulator. The software was used to model an infinite array of elements. This procedure assumes that the transmission from each individual element surrounded by elements of different sizes can be approximated by the transmission of an infinite array of identical elements. An infinite array was modeled to simulate a single element enclosed within the appropriate magnetic and electric waveguide boundary conditions, as shown in Fig.5. A plane wave was used as the excitation of a two-dimensional infinite array of similar elements. In this simulation, lossless materials were assumed and only normal incidence was considered for a

linearly polarized incident wave. The simulation results have achieved a 360° of phase agility with less than 3.8 dB of variation in transmission magnitude throughout the tuning range as shown in Fig. 6. The results are validated by a good agreement compared with that calculated by the finite integration technique.

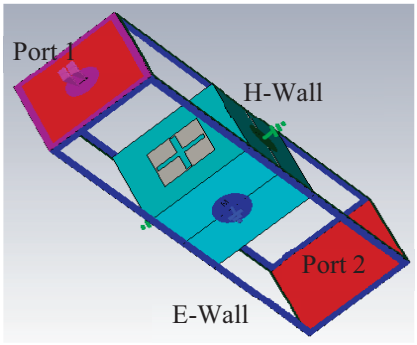

Fig. 5. Structure of waveguide simulator.

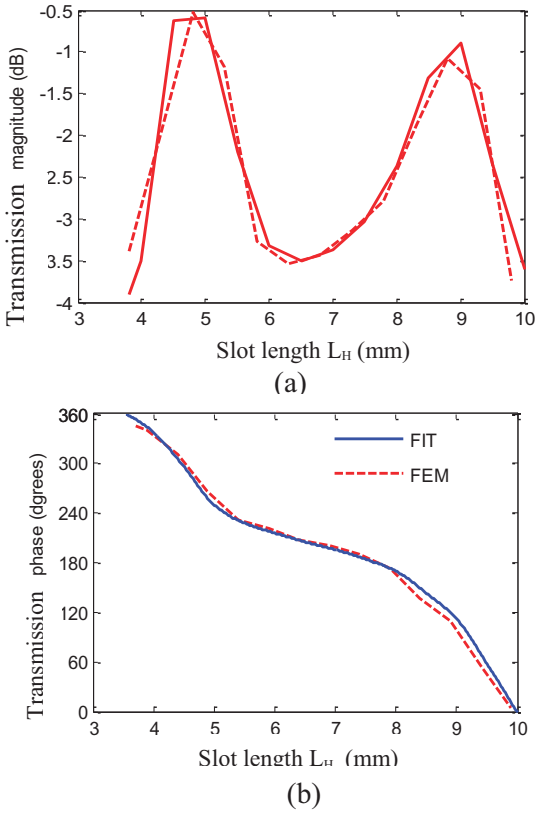

Fig. 6. Transmission (a) magnitude and (b) phase versus slot length L_H with $L_V = 0$, at f = 12 GHz.

Figure 7 illustrates the transmission coefficient magnitude and phase for different values of the slot length L_V. It shows that the transmission coefficient can be tuned by varying the slot length L_H without being really affected by the cross slot length L_V. This behavior demonstrates that two orthogonal linear polarizations can be controlled independently by the two orthogonal slots. A transmitarray composed of 17×17 elements with fixed dimension (L) of 13 mm and covering an area of 221 mm × 221 mm was designed and simulated.

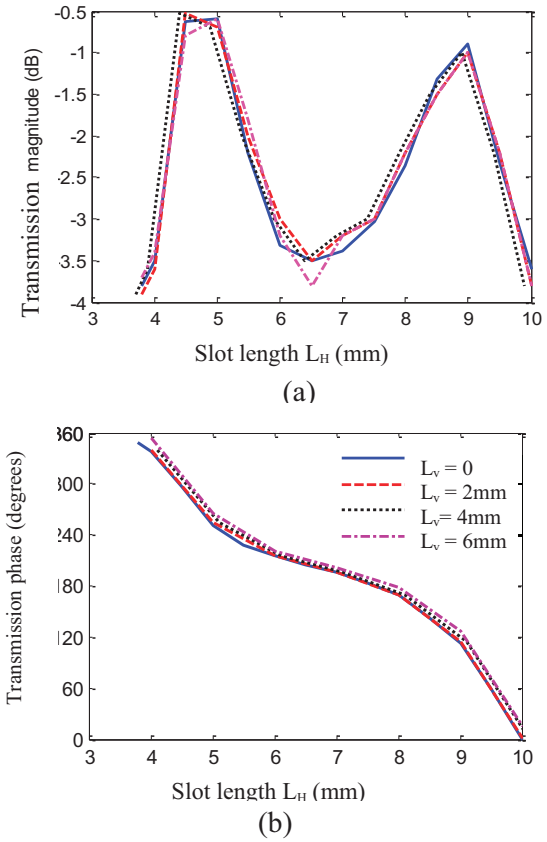

Fig. 7. Transmission (a) magnitude and (b) phase versus slot length L_H with several L_V at f = 12 GHz.

A circular horn was used as the feed, with focal length to diameter ratio, F/D, set to 1.0 to decrease the level of the sidelobes in the radiation pattern. The transmitting horn antenna illuminates one side of the transmitarray. The feed horn was positioned such that the transmitarray was prime-focus fed. This feed position provides an illumination level at the transmitarray edges of -10 dB for E-plane and -9 dB for H-plane at 12 GHz. The feed horn was 60 mm long, with an aperture radius of 25mm. Two

separate feeding pins are used to excite the horn antenna for V and H polarizations. A schematic of the transmitarray configuration showing the feed is shown in Fig. 8.

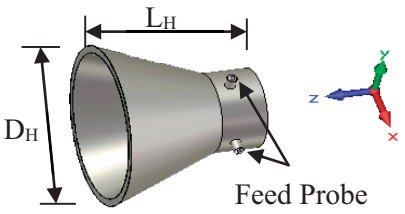

(a) Horn structure

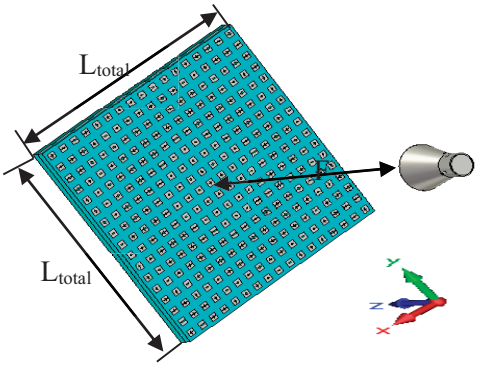

(b) 3-D transmitarray view

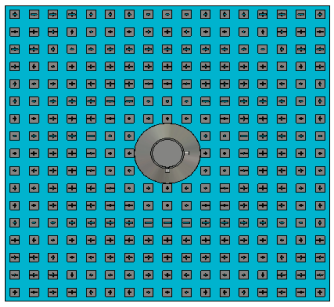

(c) Top view

Fig. 8. Transmittarray layout fed with circular horn antenna.

To design transmitarray elements; the phase of the transmitted wave should have a progressive variation over the whole surface. This implies that phases in the whole range from 0° to 360° should be used for the transmission coefficient with minimum insertion loss through the structure. The transmitarray is designed for linear polarization in the two cases of H-polarization (with the electric field on the direction of x axis) and V-polarization (with the electric field on the direction of the y-axis). The beam shaping for each polarization is achieved by adjusting the phase of the transmitted coefficient at each element independently for each linear polarization. The required phase shift for each polarization was realized by adjusting the slot length that is either L_V or L_H. Figure 9 (a) shows the distribution of the slot length L_V for horizontal polarization while Fig.9 (b) shows the distribution of the slot length L_H for the vertical polarization. Figure 9 (c) shows the variation of the cross slot lengths for vertical and horizontal polarizations along the transmitarray elements.

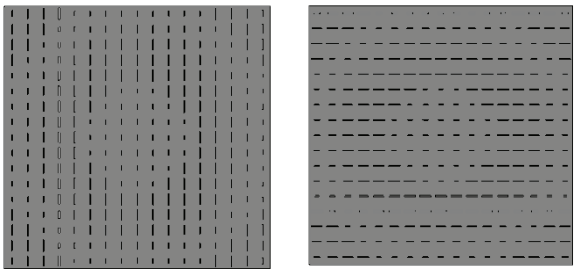

(a) L_V for horizontal (b) L_H for vertical

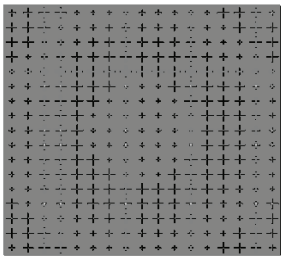

(c) Cross slot lengths

Fig. 9. Slot lengths for vertical and horizontal polarization.

As the total structure of the transmitarray is very large, simulation with the FEM requires a huge memory size, which is difficult. Consequently, the transmitarray was modeled and simulated only by FIT method. For V-polarization, computed radiation patterns components (co-polar and cross-polar) are shown in Fig. 10 at the operating frequency 12 GHz. Very high isolation between polarizations is achieved. The first sidelobe levels in the E- and H-planes are approximately 12 dB and 11.2 dB below the main peaks, respectively. The gain as a function of frequency is shown in Fig. 11. A 7.5 % bandwidth (0.9 GHz) is achieved with 1 dB gain variations. The simulated results for the H-

polarization are shown in Fig. 12. The gain as a function of frequency is depicted in Fig. 13. The performances for the V and H polarizations are almost identical.

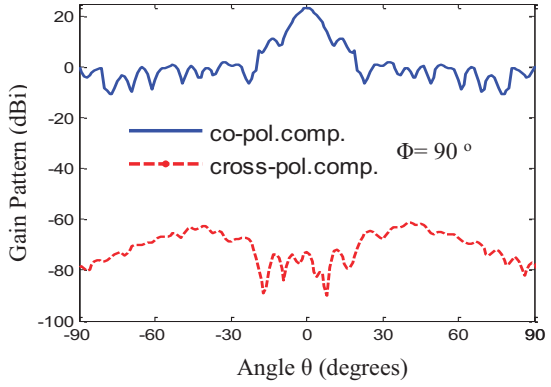

(a) E- plane

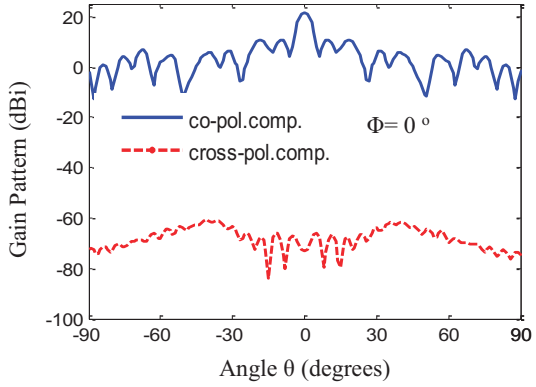

(b) H-plane

Fig. 10. E-plane and H-plane pattern plot for a boresight 17 × 17 transmitarray at 12 GHz for V-polarization.

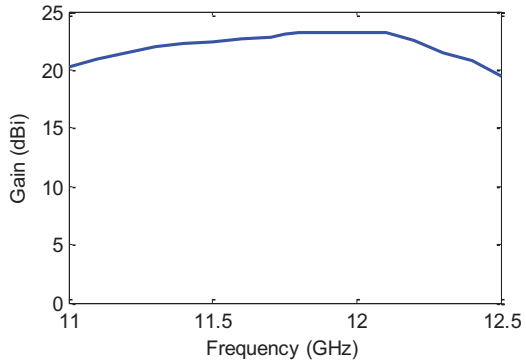

Fig. 11. 17×17 Transmittarray peak gain versus frequency for V-polarization.

B. Case B: Dual-polarization dual-band transmitarray

In this case, the transmitarray has been designed to produce a focused beam at 17.5 GHz for V-polarization and also at 12 GHz for H-polarization for satellite applications. Each polarization is controlled by adjusting the cross slots lengths, L_V and L_H, respectively according to the frequency of operation for each polarization. The range of the slot length L_V is changed as shown in Fig. 14. The slot width W_V = 0.5 mm and W_H = 0.7 mm in this case are used to get the phase transmission curve covering the range of 360° phase shift. The cross slots lengths for vertical and horizontal polarizations for each array element are shown in Fig.15. E-plane and H-plane far-field patterns of the transmitarray at 12 GHz and 17.5 GHz are depicted in Fig.16. The gains versus frequency in the two bands are illustrated in Fig. 17.

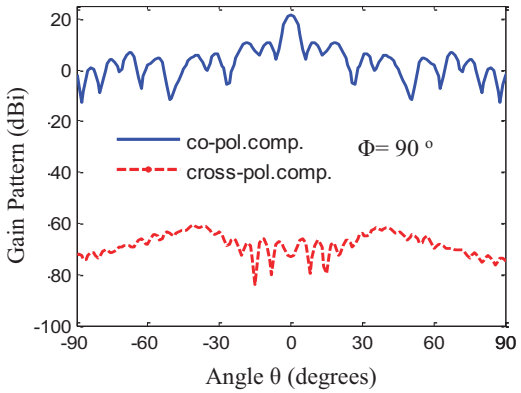

(a) E- plane

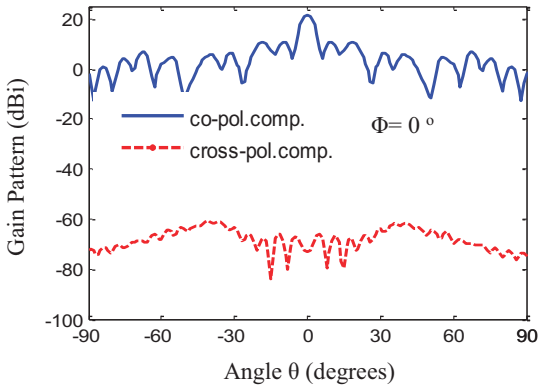

(b) H-plane

Fig. 12. E-plane and H-plane pattern plot for a boresight 17 × 17 transmitarray at 12 GHz for H-polarization.

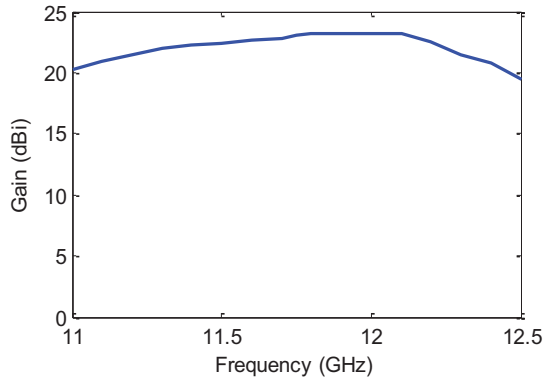

Fig. 13. 17×17 Transmittarray peak gain versus the frequency for H-polarization.

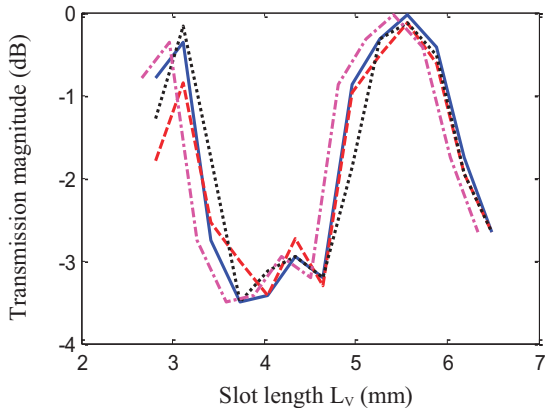

(a)

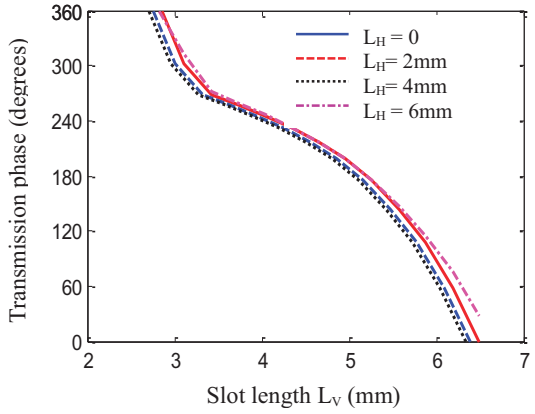

(b)

Fig. 14. Transmission (a) magnitude and (b) phase versus slot length L_V with several L_H at f = 17.5 GHz.

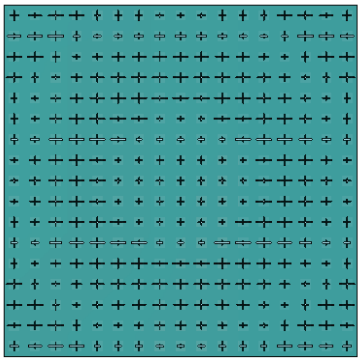

Fig. 15. Cross slots lengths for vertical and horizontal polarizations.

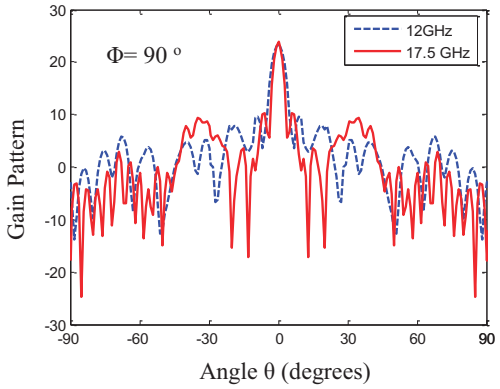

(a) E- plane

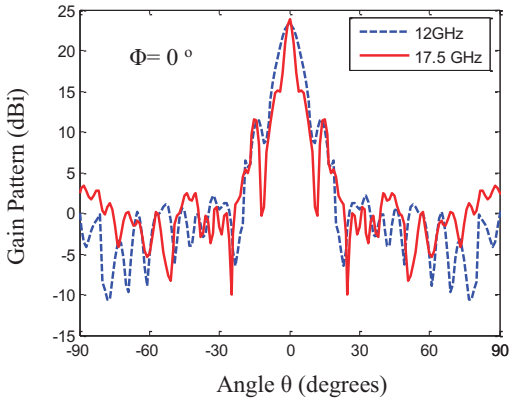

(b) H-plane

Fig.16. E-plane pattern plot for a boresight 17 ×17 transmitarray.

The vertical polarization here is operating at a higher frequency relative to that for the horizontal polarization. Thus, using the same overall dimensions of the array the beamwidth for the higher operating frequency (V-polarization) is narrower than that for the lower frequency (H-polarization). Also, the width of the slots for the

higher operating frequency has been selected narrower than that for the lower operating frequency. This variation in slot width resulted in a narrower bandwidth as shown in Table II.

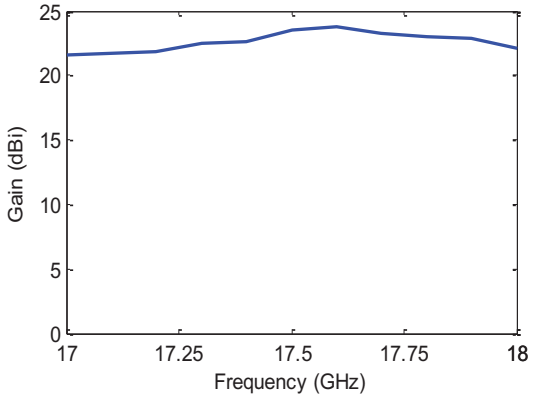

Fig. 17. 17×17Transmittarray peak gain versus frequency.

Table II: compare the radiation characteristics for H-polarization and V-polarization.

	Gain (dB)	**BW (GHz)**	**Beam width**
Horizontal polarization (x-polarized)	23.2	0.9 (7.5%)	5°
Vertical polarization (y-polarized)	23.9	0.75 (4.28%)	4°

IV. CONCLUSION

The design and analysis of a dual-polarization dual-band transmitarray were presented in this paper. Two cases are considered, transmitarray, for vertical and horizontal linear polarization at 12 GHz for case A, while another one designed at two center frequencies, 17.5 GHz for vertical polarization and 12 GHz for horizontal polarization in case B. The transmitarray consists of 17×17 elements. The radiation patterns for each polarization are achieved by adjusting the phase of the transmission coefficient at each transmitarray unit cell independently for each polarization. The slot lengths are used to control the transmission phase. Full-wave analysis using the finite element method is applied. The results are validated by comparing with that calculated by the finite integration technique. Good agreement was shown.

REFERENCES

[1] C. Ryan, J. Bray, and Y. Antar, "A broadband transmitarray using double square ring elements,"*13th International Symposium on Antenna Technology and Applied Electromagnetics and the Canadian Radio Science Meeting (ANTEM/URSI)*,Toronto, Canada, pp. 1-4, 2009.

[2] J. Huang and J. Encinar, *ReflectarrayAntennas*, John Wiley and Sons, Inc., Hoboken, NJ, USA, 2007.

[3] K. Lam, S. Kwok, Y. Hwang, and I. Lo, "Implementation of transmitarray antenna concept by using aperture coupled microstrip patches,"*Asia Pacific Microwave Conference*, *APMC*,Hong Kong, pp.433- 436, 1997.

[4] H. Son and W. Zhang, "Design of broadband element of transmitarray with polarization transform,"*International Workshop on Small and Smart Antennas, Metamaterials and Applications (IWAT '07)*, pp. 287-290, Cambridge, UK, 2007.

[5] S. Zainud-Deen, S. Gaber, H. Malhat, and K. Awadalla, "Multilayer dielectric resonator antenna transmitarray for near-field and far-field fixed RFID reader,"*Progress In Electromagnetics Research C, PIER C*, vol. 27, pp. 129-142, 2012.

[6] J. Encinar, L. Datashvili, J. Zornoza, M. Arrebola, M. Sierra-Castaner, J. Besada-Sanmartin, H. Baier, and H. Legay, "Dual-polarization dual-coverage reflectarray for space applications,"*IEEE Transaction on Antennas and Propagation,* vol.54, no.10, pp.2827-2836, Oct. 2006.

[7] A. Abd-Elhady, S. Zainud-Deen, A. Mitkees, and A. Kishk, "Dual polarized dual feed aperture-coupled DRA reflectarray,"*29th National Radio Science Conference (NRSC 2012), Faculty of Engineering, Cairo University*, Cairo, Egypt, pp. 97-102, 2012.

[8] D. Cadoret, L. Marnat, R. Loison, R. Gillard, H. Legay, and B. Salome, "A dual linear polarized printed reflectarray using slot loaded patch elements,"*The second European Conference Antenna and Propagation (EUCAP* 2007), pp. 1-5, 2007.

[9] D. Hutton, Fundamentals of Finite Element Analysis, *McGraw-Hills Companies*, USA, 2004.

[10] S. Cooke, R. Shtokhamer, A. Mondelli, and B. Levush, "A finite integration method for conformal, structure-grid, electromagnetic simulation,"*Journal of computational physics*, vol.215, pp. 321-347, 2006.